Video Article

Applicability Analysis of Assessment Methods for Morphological Parameters of Corroded Steel Bars

Dawang Li[1,2], Ping Li[1,2], Yingang Du[3], Ren Wei[1,2]

[1]Department of Civil Engineering, Shenzhen University

[2]Guangdong Province Key Laboratory of Durability for Marine Civil Engineering, Shenzhen University

[3]Department of Engineering and the Built Environment, Anglia Ruskin University

Correspondence to: Yingang Du at yingang.du@anglia.ac.uk, Ren Wei at 2150150409@email.szu.edu.cn

URL: https://www.jove.com/video/57859
DOI: doi:10.3791/57859

Keywords: Engineering, Issue 141, Mass loss, Vernier calipers, Drainage, XCT, 3D scanning, corrosion, spatial variability

Date Published: 11/1/2018

Citation: Li, D., Li, P., Du, Y., Wei, R. Applicability Analysis of Assessment Methods for Morphological Parameters of Corroded Steel Bars. *J. Vis. Exp.* (141), e57859, doi:10.3791/57859 (2018).

Abstract

The irregular and uneven residual sections along the length of a corroded steel bar substantially change its mechanical properties and significantly dominate the safety and performance of an existing concrete structure. As a result, it is important to measure the geometry and amount of corrosion of a steel bar in a structure properly to assess the residual bearing capacity and service life of the structure. This paper introduces and compares five different methods for measuring the geometry and amount of corrosion of a steel bar. A single 500 mm long and 14 mm diameter steel bar is the specimen that is subjected to accelerated corrosion in this protocol. Its morphology and the amount of corrosion were carefully measured before and after using mass loss measurements, a Vernier caliper, drainage measurements, 3D scanning, and X-ray micro-computed tomography (XCT). The applicability and suitability of these different methods were then evaluated. The results show that the Vernier caliper is the best choice for measuring the morphology of a non-corroded bar, while 3D scanning is the most suitable for quantifying the morphology of a corroded bar.

Video Link

The video component of this article can be found at https://www.jove.com/video/57859/

Introduction

Corrosion of a steel bar is one of the principal reasons for deterioration of a concrete structure and is caused by concrete carbonation and/or chloride intrusion. In concrete carbonation, corrosion tends to be generalized; while in chloride intrusion, it becomes more localized[1,2]. No matter what the causes are, corrosion cracks the concrete cover from radial expansion of corrosion products, deteriorates the bond between a steel bar and its surrounding concrete, penetrates the bar surfaces, and decreases the bar cross-sectional area considerably[3,4].

Due to the non-homogeneity of structural concrete and variations in the service environment, corrosion of a steel bar occurs randomly over its surface and along its length with great uncertainty. Contrary to the generalized uniform corrosion caused by concrete carbonation, the pitting corrosion caused by chloride intrusion causes attack penetration. Furthermore, it causes the residual section of a corroded bar to vary considerably among the bar surface and length. As a result, the bar strength and bar ductility decrease. Extensive research has been performed to study the effects of corrosion on mechanical properties of a steel bar[5,6,7,8,9,10,11,12,13,14,15]. However, less attention has been given to the measurement methods of morphological parameters and corrosion characteristics of steel bars.

Some researchers have used mass loss to evaluate the amount of corrosion of a steel bar[5,10,11,14]. However, this method can only be used to determine the average value of the residual sections and cannot measure the distribution of the sections along its length. Zhu and Franco have improved this method by cutting a single steel bar into a series of short segments and weighing each segment to determine variations of the areas of the residual sections along its length[13,14]. However, this method causes extra loss of the steel material during the cutting and cannot touch the minimum residual section of the corroded bar exactly, which dominates its bearing capacity. A Vernier caliper is also used to measure the geometric parameters of a steel bar[14,15]. However, the residual section of a corroded bar is very irregular, and there is always a significant deviation between the measured and actual sectional dimensions of a corroded bar. Based on Archimedes' principle, Clark *et al.* adopted the drainage method to measure the residual sections of a corroded bar along its length, but displacement of the bar was manually controlled without significant accuracy in this case[11]. Li *et al.* improved this drainage method by using an electric motor to automatically control the displacement of a steel bar and measure results more accurately[16]. Finally, over the past few years, with the development of 3D scanning technology, this method has been used to measure the geometric dimensions of a steel bar[17,18,19,20]. Using 3D scanning, the diameter, residual area, centroid, eccentricity, moment of inertia, and corrosion penetration of a steel bar can be precisely acquired. Although researchers have used these methods in different experimental settings, there has not been a comparison and evaluation of the methods with respect to their precision, suitability and applicability.

Corrosion, particularly pitting corrosion, compared to generalized corrosion, not only changes the mechanical properties of corroded bars but also decreases the residual bearing capacity and service life of concrete structures. More accurate measurements of morphological parameters of corroded steel bars for the spatial variability of corrosion along bar length are imperative for more reasonable assessments of bar mechanical properties. This will help evaluate the safety and reliability of reinforced concrete (RC) structures damaged by corrosion more precisely[21,22,23,24,25,26,27,28,29].

This protocol compares the five discussed methods for measuring the geometry and amount of corrosion of a steel bar. A single, 500 mm long and 14 mm in diameter, plain round bar was used as the specimen and subjected to accelerated corrosion in the lab. Its morphology and level of corrosion were carefully measured before and after using each method, including mass loss, a Vernier caliper, drainage measurements, 3D scanning, and X-ray micro computed tomography (XCT). Finally, the applicability and suitability of each were evaluated.

It should be noted that the ribbed bars embedded in concrete, not the plain bars exposed to air, are commonly used in concrete structures and subjected to corrosion. For ribbed bars, the Vernier caliper may not be as easily applied. Because these bars corrode in concrete, their surface penetration is more irregular compared to bars exposed to air[11]. However, this protocol is geared towards the applicability of analysis of different measurement methods on the same bar; therefore, it uses a naked plain bar as the specimen to eliminate the influence of ribs and concrete non-homogeneity on morphological parameter measurements. Further work on the measurement of corroded ribbed bars using other methods may be carried out in the future.

Protocol

1. Testing the Specimen and the Manufacturing Process

1. Acquire a 500 mm long, 14 mm diameter plain steel bar (grade Q235) for the manufacturing of the test specimens.
2. Polish the surface of the bar using a fine sandpaper to remove the mill scales on the surface.
3. Cut the bar at 30 mm and 470 mm from its left end, as shown in **Figure 1,** using a cutting machine.
4. Measure the weights of the three bar specimens, using a digital electronic scale.
5. Measure the diameters of the three specimens using the five methods described in step 2, and record the results of the non-corroded bar specimens.
6. Corrode the 440 mm bar specimen using the electrochemical method, as detailed below:
    1. Cover 70 mm of each end firmly with insulation tape. Attach an electrical wire to one end of the 440 mm bar specimen.
    2. Mix an adhesive with a hardener in a 1:1 proportion to make epoxy resin. Apply the epoxy resin on the insulated 70 mm ends of the bar specimen uniformly to protect both ends from corrosion.
    3. Place the 440 mm long bar specimen into a plastic water tank that contains 3.5% NaCl as an electrolyte and a copper plate as a cathode.
    4. Connect one end of the bar specimen as a node to the positive pole and the cathode copper plate to the negative pole of a direct current (DC) power supplier, respectively, to set up an electrical circuit for the accelerated corrosion of the bar specimen.
    5. Switch on the DC power supply to apply a constant direct current of 2.5 μA/cm^2 onto the bar specimen for the whole period of corrosion.
    6. Switch off the current to terminate the corrosion process when the amount of corrosion of the bar specimen reaches the anticipated level of corrosion, as estimated using Faraday's law.
    7. Place the above corroded bar specimen into a 12% HCl solution tank for 30 minutes to remove the corrosion products from its surface. Immerse the acid-cleaned bar specimen into a saturated lime water tank for neutralization and further clean using tap water.
    8. Dry the above cleaned corroded bar specimen in air. Mark its surface for the measurement.
7. Measure the morphological parameters and corrosion amount of the corroded bar specimen.
    NOTE: Cleaning does affect the mass loss of a corroded steel bar. Different types of acid solution and the different times of immersion in the acid solution would cause different amounts of mass loss. In this test, however, no comparison was made between different cleaning techniques, For consistency, the cleaning process follows the China National Standard for test methods of long-term performance and durability of ordinary concrete[30].

2. Measurement Methods and Procedures

1. **Mass loss method**
    1. Place an electronic scale on a horizontal platform and zero it.
    2. Place the polished bar specimen before corrosion horizontally onto the electronic scale and take a reading from the scale as the mass of a non-corroded steel bar m_0 **(g)**.
    3. Place the cleaned bar specimen after corrosion horizontally onto the electronic scale and take a reading from the scale as the mass of the corroded steel bar m_c **(g).**
    4. Calculate the amount of corrosion of the bar using an equation of $Q_{cor}= (m_c-m_0)/m_0 \times 100\%$.
    5. Calculate the average area of the residual section of the corroded bar specimen using an equation $A_{sc}=A_{s0}(1-Q_{cor})$, where, A_{s0} is the area of a non-corroded steel bar.

2. **Vernier caliper method**
    1. Mark the surface of the bar specimen along its length in 10 mm intervals from the left end of the bar using a marker pen, as shown in **Figure 1**.
    2. Move the Vernier scale of the caliper to its original position. Make the two jaws touch each other and line up the two zero lines of the Vernier and main scales. Then push its zero button to zero the Vernier scale.

3. Place the Vernier caliper across the diameter of the bar specimen. Move the Vernier scale to make its two jaws touch the bar surface gently. Measure the diameter of the bar specimen at the marked section and at the given angle.
4. Repeat step 2.2.3 four times to measure the bar diameters at the marked section and at angles of 0°, 45°, 90° and 135°, respectively, as shown in **Figure 2.**
5. Average the above four measured diameters and take it as the representative diameter D_i **(mm)** of the bar specimen at the marked section.
6. Calculate the cross-sectional area of the bar specimen at the marked section using an equation $A_i=pD_i^2/4$ (mm^2).
7. Repeat steps 2.2.3 to 2.2.6 for all the marked sections of the bar specimen to measure the distribution of its cross sections along its length after corrosion.

3. **Drainage method**
   1. Set up the electromechanical universal testing (EUT) machine, as shown in **Figure 3**.
   2. Place a glass container under the head of the EUT machine and pour tap water into the container until the water level reaches the outlet.
   3. Place a 200 mL beaker on the platform of an electronic scale right below the outlet of the glass container.
   4. Clamp one end of the bar specimen using the head of the EUT machine vertically.
   5. Switch on the EUT machine to move its head down slowly until the other end of the bar specimen just touches the top surface of the water in the container.
   6. Take the initial reading of the electronic scale as M_i.
   7. Run the EUT machine to move the bar specimen down into the water in the container at a rate of 1.0 mm/min.
   8. Take the final reading of the electronic scale as M_{i+1} for the mass of the water that has been discharged from the container due to the 10 mm displacement of the bar specimen into the water in the container.
   9. Assume the cross-section of the 10 mm displaced bar specimen is uniform, calculate the cross-sectional area of the h=10 mm displaced bar using the equation of $A_i= (M_{i+1} - M_i)/(\rho h)$, where $(M_{i+1} - M_i)$ is the measured mass of the water discharged from the container for the 10 mm displaced bar specimen. ρ=1,000 kg/m^3 is the density of water.
   10. Repeat steps 2.3.6 to 2.3.9 for each 10 mm long displaced bar specimen until displacing the whole length of the bar into the water to measure the distribution of bar cross sections along its length.

4. **3D scanning method**
   1. Spray white developer on the surface of the bar specimen and dry it in air. Place it horizontally onto the platform of a 3D scanner, as shown in **Figure 4**.
   2. Calibrate the position of the bar specimen on the platform of the 3D scanner by randomly making white small dots on label paper for the 3D reconstruction of the bar specimen.
   3. After launching the 3D scanner and the corresponding data extraction software, scan the bar specimen along its length and collect the corresponding scanned data via the 3D scanner. Use manufacturer's instructions.
   4. Develop the spatial model of the bar specimen using the software and collect the relevant date files.
   5. Place the developed spatial model data of the bar specimen and two self-compiled MATLAB programs in the same folder of a computer.
   6. Run the first MATLAB program on the developed spatial model data of the bar specimen to generate the relevant MAT file. Save the obtained MAT file in the same folder.
   7. Run the second MATLAB program on the above obtained MAT file to generate the relevant morphological data of the bar specimen, including sectional area, moment of inertia, polar moment of inertia, eccentric distance etc.

5. **XCT method**
   NOTE: After the four measurements on the 440 mm long bar specimen, the fifth measurement was done on the 30 mm long bar specimens using the XCT method due to its bar length limitation.
   1. Cut a 30 mm bar specimen from both ends of a 500 mm long steel bar and from the 440 mm long corroded steel bar, as shown in **Figure 1.** Use them as the non-corroded and corroded bar specimens, respectively.
   2. Place the bar specimens onto the rotatable platform of the XCT instrument, as shown in **Figure 5**. Close the door of the XCT instrument. The bar specimen is sandwiched between the radioactive source and the signal receiver of the XCT instrument.
   3. Run the XCT operation software installed on a computer to set up shooting parameters. Adjust the bar specimen to the shooting position.
   4. Set up the pixel size and magnification factor in the "image control" table of the XCT instrument operation software.
   5. Run the XCT instrument by clicking the **Start** button to scan the bar specimen. Collect the scanned data of bar specimen.
   6. Run the software package on the above scanned data to produce the geometric parameters of the bar specimen accordingly.

Representative Results

Figure 6 shows the diameters of the 500 mm long non-corroded bar specimen at angles of 0°, 45°, 90°, and 135° for each section along its length measured using Vernier calipers. The bars were then cut into three parts, as shown in **Figure 1**.

Figure 7 presents the cross-sectional areas of the non-corroded bar specimens along its lengths measured using four and five methods, respectively, for the 440 mm long middle part and for the 30 mm long end.

Figure 8 shows the spatial images and three cross-sections of the corroded bar specimen measured using 3D scanning and XCT methods, respectively.

Figure 9 reports the cross-sectional areas of the corroded bar specimen along its length measured using four and five methods for the 300 mm and the 30 mm long specimens.

Table 1 summarizes the diameters of the 30 mm long non-corroded bar specimen measured using the calipers, the 3D scanning and the XCT methods.

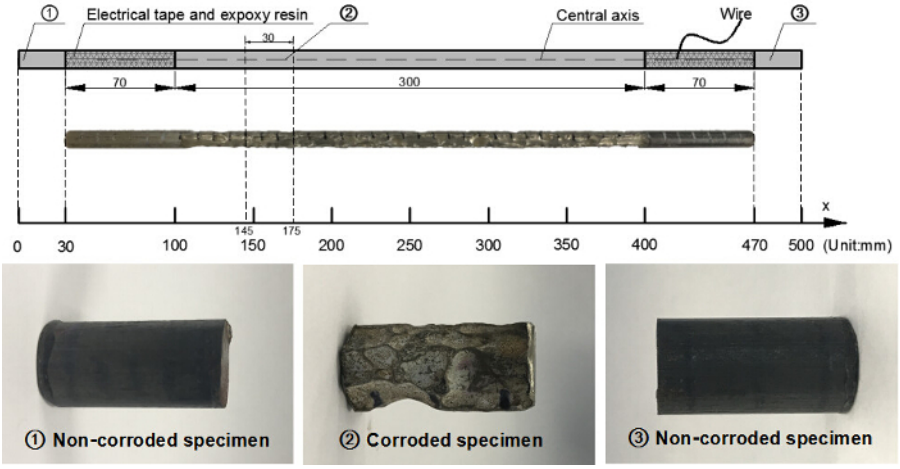

Figure 1: Steel bar specimen. Figure 1 shows the details of the bar specimens. Two 30 mm long end parts ① and ③ were used as the non-corroded specimens. The 440 mm long middle part ② was used as the corroded bar specimen. The three parts were cut from the 500 mm long steel bar at distances of 30 mm and 470 mm, respectively, from the left end of the steel bar. This figure has been modified from Figures 1 and 2 by Li, *et al.*[16]. Please click here to view a larger version of this figure.

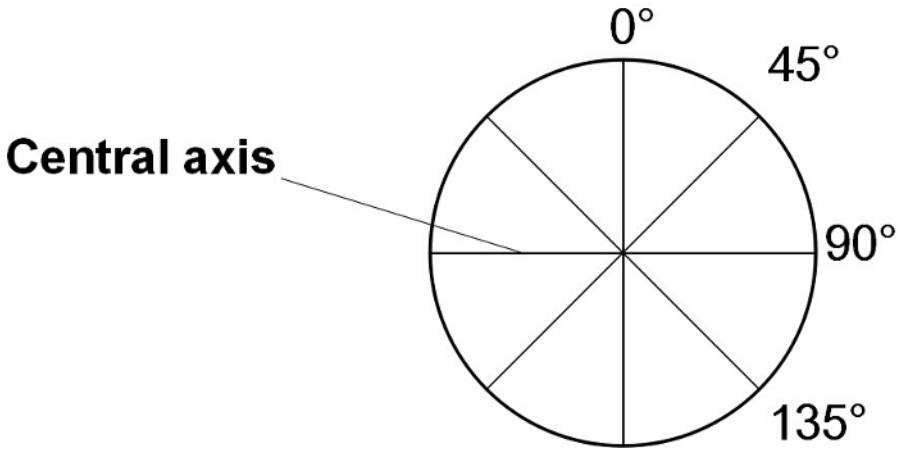

Figure 2: Angles of bar diameter measurement using Vernier caliper. This shows the angles of bar diameter measurement using the Vernier caliper at each cross-section along the bar length. This figure has been modified from **Figure 3** by Li, *et al.*[16]. Please click here to view a larger version of this figure.

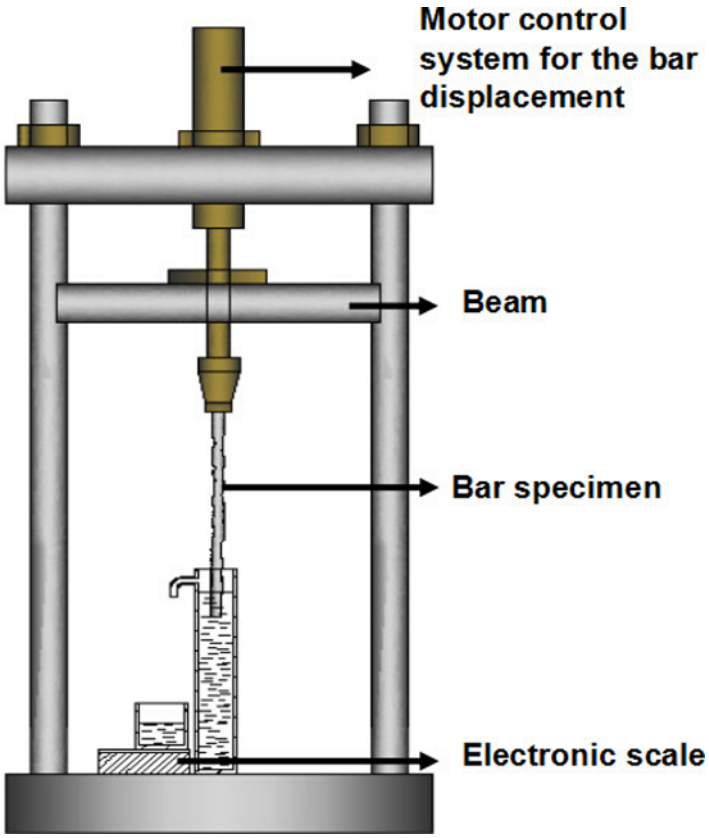

Figure 3: Device for the drainage method. This shows the electromechanical universal testing machine (EUT) for the drainage method. This figure has been modified from **Figure 4** by Li, *et al.*[16]. Please click here to view a larger version of this figure.

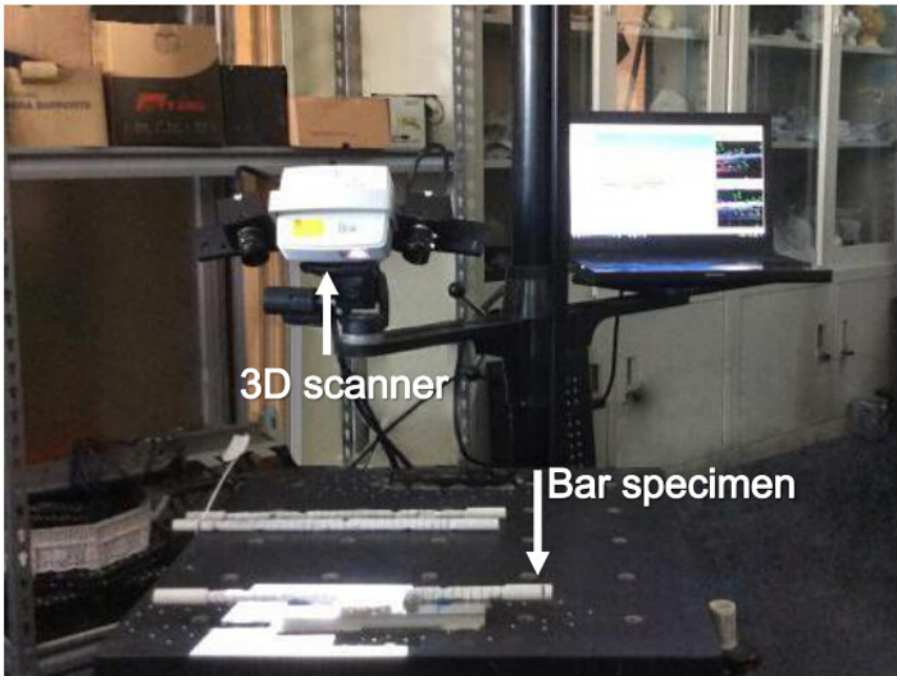

Figure 4: Device of 3D Scanning and marked bar specimens. This shows the device of 3D scanning and the marked bar specimens to be scanned. This figure has been modified from **Figure 5** by Li, *et al.*[16]. Please click here to view a larger version of this figure.

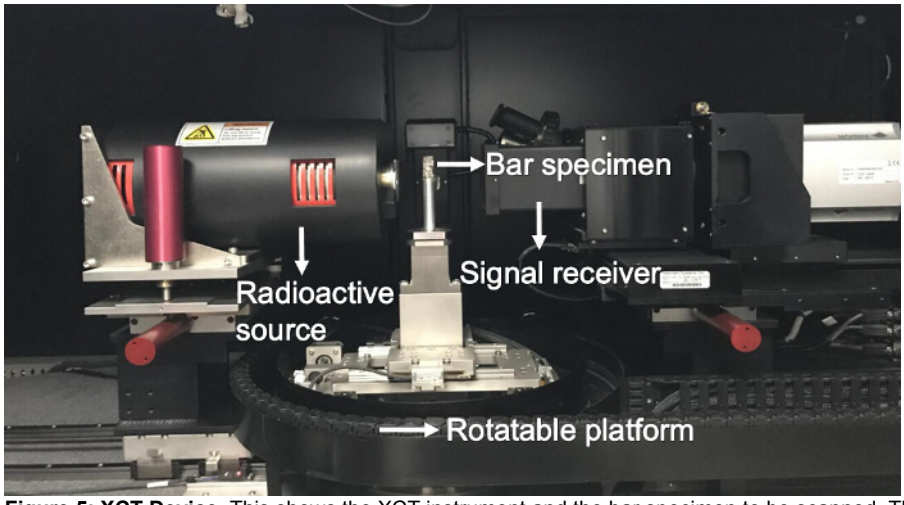

Figure 5: XCT Device. This shows the XCT instrument and the bar specimen to be scanned. This figure has been modified from **Figure 7** by Li, *et al.*[16]. Please click here to view a larger version of this figure.

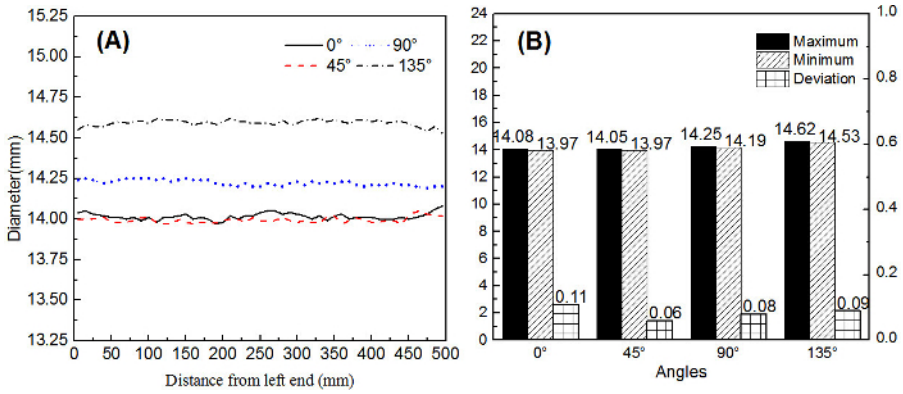

Figure 6: The measured diameters of the 500 mm long non-corroded bar using the Vernier caliper. This shows the diameters of the 500 mm long non-corroded bar measured using the Vernier caliper. **Figure 6A** shows the diameters measured at four different angles in each section along the bar length. **Figure 6B** presents the maximum, minimum and deviation of the measured diameters at four different angles. This figure is reprinted from **Figure 8** by Li, *et al.*[16]. Please click here to view a larger version of this figure.

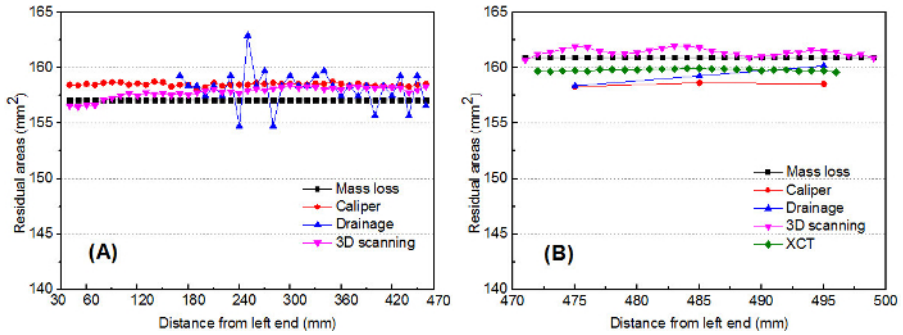

Figure 7: The measured sectional areas of the non-corroded bar specimen along its length. Figure 7A shows the measured sectional areas of the 440 mm long bar specimen along its length before its corrosion. **Figure 7B** shows the measured sectional areas of the 30 mm long non-corroded end bar specimens. This figure is reprinted from **Figure 9** by Li, *et al.*[16]. Please click here to view a larger version of this figure.

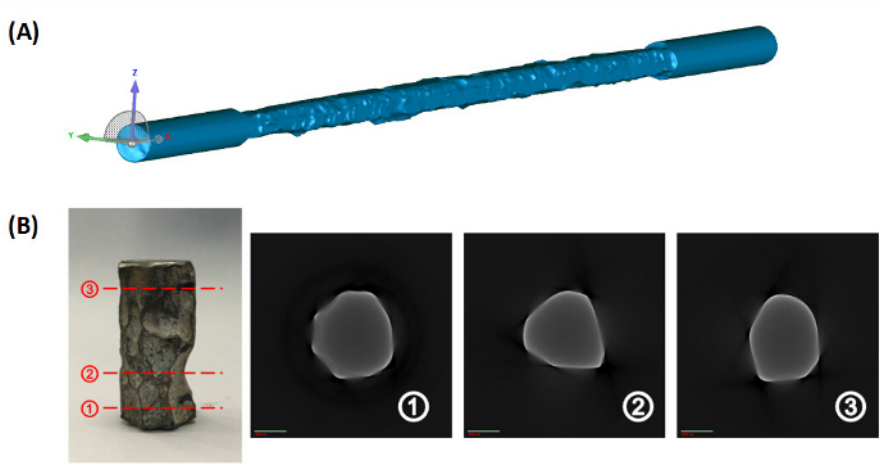

Figure 8: The spatial images and three cross section of the corroded bar specimen measured using 3D scanning and XCT method. **Figure 8A** shows the spatial images of the 440 mm long corroded bar specimen measured using 3D scanning. **Figure 8B** presents the images of three cross sections of the corroded bar specimen measured using the XCT method. This figure has been modified from Figures 10 and 11 by Li, *et al*.[16]. Please click here to view a larger version of this figure.

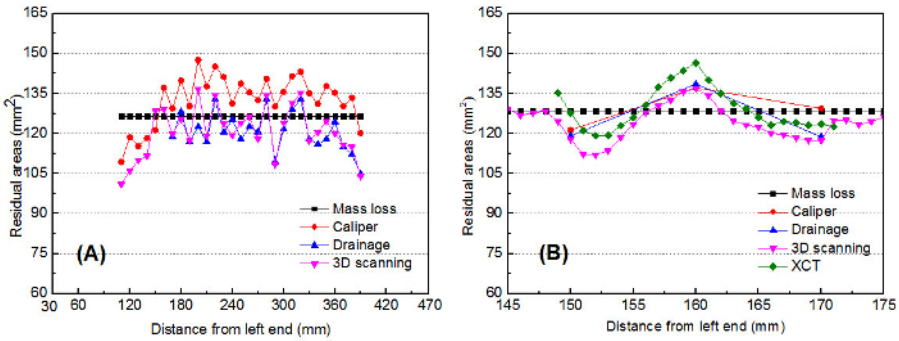

Figure 9: The measured sectional area of the corroded bar specimen along its length. **Figure 9A** shows the measured sectional area of the 300 mm long corroded bar specimen along its length. **Figure 9B** reports the measured areas of the 30 mm long corroded bar specimen. This figure has referred to Figures 12 and 13 by Li, *et al*.[16] Please click here to view a larger version of this figure.

Diameter (mm)	Caliper method	XCT method	3D scanning method
Maximum	14.22	14.27	14.34
Minimum	14.19	14.26	14.31
Deviation	0.03	0.01	0.03

Table 1: The measured diameters of the 30 mm long non-corroded bar specimen using caliper, 3D scanning and XCT methods. This summarizes the maximum and minimum diameters of the 30 mm long non-corroded bar specimens measured using three methods. This figure has been modified from Table 1 by Li, *et al*.[16].

Discussion

Figure 6A and **6B** show that the measured diameters of the non-corroded bar specimen do not vary significantly along its length. The maximum difference between the measured diameters along the bar length is only about 0.11 mm with a maximum deviation of 0.7%. This indicates that the geometry of a non-corroded bar can be well evaluated using a Vernier caliper. However, the measured diameters at different angles of the same cross-section differ consistently and considerably from each other. For the given bar specimen, the maximum and minimum diameters of 14.62 mm and 14.05 mm occur at angles of 45° and 135° with a maximum deviation of 4%. In other words, the cross-section of a non-corroded bar is not perfectly circular, but elliptical. Hence, attention should be paid to the measurement of the bar diameter when the actual cross-sectional area is calculated directly based on the measured diameter of the steel bar.

In addition to the measurement of the plain bar diameter using Vernier calipers, we also used XCT and 3D methods to measure the cross section of a rib bar, for which Vernier calipers cannot be used easily. We found different diameters at different angles for the rib bar as well. The plain bar specimen is used in this paper since it can be measured using all five different methods for comparison.

The steel bars in concrete structures are mainly in tension or in compression. Hence, for the given strength, the bearing capacity of a steel bar depends on its cross sectional area. Assuming that there is 4.0% difference between the maximum and the minimum bar diameter at the different angles and the bar cross section is elliptical, its area is calculated by $A=\pi(d-0.04d)(d+0.04d)/4=0.998\pi d^2/4$ with a 0.016% difference of

bar area for the given 4.0% difference of bar diameter. Hence, because of the different diameters at different angles, the bar cross-sectional area decreases. However, this bar sectional area difference seems less significant, compared with the bar diameter difference in the same section.

Figure 7A and **7B** show that the sectional areas of the non-corroded bar measured using the methods of mass loss, caliper measurements, 3D scanning and XCT do not vary significantly from one method from another, except for some points measured using the drainage method. This was because there were some uncertainties using the drainage method, such as surface tension of a water bulb, bond action between water and the tube, and the moisture content of a bar surface. For example, if the bar surface is too dry when it is displaced into the water container, it would absorb some water first before discharging water from the container. If the surface tension of a water bulb is greater than 90° when it flows through a tube, less water can be discharged from the container via the glass tube for the first 10 mm displaced bar. As a result, the amount of corrosion of the bar specimen would be over-estimated and the actual residual area of the corroded bar would be under-estimated. As the bar specimen continues to move into the container, the pressure builds up in the tube until the friction resistance between the water and tube surface is overcome; thus, much more water would be discharged for the consequent 10 mm displaced bar specimen into the container. As a result, the amount of corrosion of the bar specimen would be under-estimated and the actual residual area of the corroded bar would be over-estimated. This is the reason why the measured area of the bar specimen using the drainage method is less stable and consistent compared with those measured by other methods.

In addition, **Table 1** also shows that the diameters of the 30 mm long non-corroded bar specimen measured using the Vernier caliper, the 3D scanning and XCT method are close to each other. Therefore, the four methods of mass loss, caliper measurement, 3D scanning and XCT method can be used to define the sectional characteristics of a non-corroded steel bar more precisely.

Furthermore, through a comprehensive comparison of the used instruments, test costs, efficiency, measurement accuracy of the above four different methods, it becomes clear that the caliper method is the most suitable for the measurement of morphology of a non-corroded steel bar because of its simplicity, high efficiency and accuracy compared to other methods.

It should be pointed out that, as shown in **Figure 1**, the cut end surfaces of both 30 mm long non-corroded bars were not perfectly planar and transversely straight. This may cause some discrepancies about the bar actual length measured using the Vernier caliper and, in turn, the deviation of the calculated sectional areas from the measured mass loss or volume variation. Hence, there are some differences of the measured sectional areas of the non-corroded bars between **Figure 7A** and **7B**.

Figure 8A and **8B** show that, due to the removal of metal from bar surface irregularly via electrochemical reaction process, the residual cross-section of the corroded bar specimen is neither circular nor elliptical. Instead, it became very irregular and varied substantially along the length of the corroded bar.

Figure 9A and **9B** show the residual areas of the cross-section of the corroded bar specimens along its length that were measured using mass loss, calipers, drainage method, 3D scanning and the XCT method. It is clear that for the corroded bar specimen, the mass loss method can only produce the average cross-sectional area of a corroded bar and remain constant along its whole length. It does not reflect the variation of the actual residual section of a corroded bar along its length, as shown in **Figure 8A** and **8B**. In addition, because a caliper cannot touch the base of pitting on the bar surface, it can only measure an equivalent diameter of a residual section of a corroded bar. Because of such an intrinsic shortcoming, the caliper method is less able to measure the morphological parameter of a corroded bar specimen precisely.

Figure 9A and **9B** also show that the residual areas of the corroded bar specimen measured using XCT and 3D scanning methods vary consistently along its length and are close to each other. However, the XCT method can only accommodate 30 mm specimens. Therefore, the XCT method cannot be widely used in practical engineering. Moreover, the use of the XCT method also imposes very strict requirements on the cutting and preparation of a bar specimen. If the section of a bar specimen is not a straight plane, but crooked or uneven, a significant deviation can be made and included in the bar sectional area measured using the XCT method. The 3D scanning method can accommodate the 440 mm long bar specimen and measure the morphology of both non-corroded and corroded specimens accurately enough. It has substantial advantages over the other four methods on precision, efficiency and applicability in the measurement of bar surface morphology. Besides, the 3D method can also generate some more useful morphological information of a bar specimen, including the depths of corrosion pits on bar surface, the moment of inertia, centroid, moments of inertia of bar section, *etc*. along its length. Hence, the 3D scanning method is the most favored option for measuring morphology of a steel bar, particularly a corroded steel bar.

From the above results and discussion, the following conclusions can be drawn. For a non-corroded steel bar, a Vernier caliper is the best tool for measuring its morphology. It not only has a high accuracy of measurement but also is most economical. Although the drainage method can measure the residual cross-sectional area of a corroded steel bar along the bar length, the accuracy of the measurement device needs further improvement. Its measured results may be affected by some uncertainties, such as the surface tension of the water bulb, the bond with the flow tube, and the moisture of bar surface, *etc*., and therefore the drainage method has to be used very carefully. Although the XCT method can accurately measure the residual section area of a corroded steel bar, the length of a steel bar it can accommodate is limited to 30 mm. The 3D scanning method has substantial advantages over the other four methods on aspects of precision, efficiency and applicability in the measurement of surface morphology of a steel bar, particularly a corroded steel bar. In addition, it can generate much more useful morphology measurements of a corroded steel bar, such as pit depth, sectional eccentricity, *etc*. It is the most optimal method for the measurement of morphological parameters of a corroded steel bar.

Disclosures

The authors have nothing to disclose.

Acknowledgements

The authors at Shenzhen University greatly acknowledge the financial support from the National Natural Science Foundation of China (Grant No. 51520105012 and 51278303) and the (Key) Project of Department of Education of Guangdong Province. (No.2014KZDXM051). They also thank the Guangdong Provincial Key Laboratory of Durability for Marine Civil Engineering, College of Civil Engineering at Shenzhen University for providing testing facilities and equipment.

References

1. Cavaco, E. S., Bastos, A., & Santos, F. A. D. Effects of corrosion on the behaviour of precast concrete floor systems. *Construction & Building Materials.* **145** (2017).
2. Cavaco, E. S., Neves, L. A. C., & Casas, J. R. On the robustness to corrosion in the life cycle assessment of an existing reinforced concrete bridge. *Structure and Infrastructure Engineering.* **14** (2), 137-150 (2017).
3. Muthulingam, S., & Rao, B. N. Non-uniform corrosion states of rebar in concrete under chloride environment. *Corrosion Science.* **93**, 267-282 (2015).
4. Apostolopoulos, C. A., & Papadakis, V. G. Consequences of steel corrosion on the ductility properties of reinforcement bar. *Construction & Building Materials.* **22** (12), 2316-2324 (2008).
5. Fernandez, I., Bairán, J. M., & Marí, A. R. Corrosion effects on the mechanical properties of reinforcing steel bars. Fatigue and σ - ε behavior. *Construction & Building Materials.* **101** 772-783 (2015).
6. Papadopoulos, M. P., Apostolopoulos, C. A., Zervaki, A. D., & Haidemenopoulos, G. N. Corrosion of exposed rebars, associated mechanical degradation and correlation with accelerated corrosion tests. *Construction & Building Materials.* **25** (8), 3367-3374 (2011).
7. Castro, H., Rodriguez, C., Belzunce, F. J., & Canteli, A. F. Mechanical properties and corrosion behaviour of stainless steel reinforcing bars. *Journal of Materials Processing Technology.* **143 - 144** (1), 134-137 (2003).
8. Almusallam, A. A. Effect of degree of corrosion on the properties of reinforcing steel bars. *Construction & Building Materials.* **15** (8), 361-368 (2001).
9. Papadopoulos, M. P., Apostolopoulos, C. A., Alexopoulos, N. D., & Pantelakis, S. G. Effect of salt spray corrosion exposure on the mechanical performance of different technical class reinforcing steel bars. *Materials & Design.* **28** (8), 2318-2328 (2007).
10. Zhang, W., Song, X., Gu, X., & Li, S. Tensile and fatigue behavior of corroded rebars. *Construction & Building Materials.* **34** (5), 409-417 (2012).
11. Clark, L. A., Chan, A. H. C., & Du, Y. G. Residual capacity of corroded reinforcing bars. *Magazine of Concrete Research.* **57** (3), 135-147 (2005).
12. Chan, A. H. C., Clark, L. A., & Du, Y. G. Effect of corrosion on ductility of reinforcing bars. *Magazine of Concrete Research.* **57** (7), 407-419 (2005).
13. Zhu, W., & François, R. Corrosion of the reinforcement and its influence on the residual structural performance of a 26-year-old corroded RC beam. *Construction & Building Materials.* **51** (2), 461-472 (2014).
14. François, R., Khan, I., & Dang, V. H. Impact of corrosion on mechanical properties of steel embedded in 27-year-old corroded reinforced concrete beams. *Materials & Structures.* **46** (6), 899-910 (2013).
15. Torres-Acosta, A. A., & Castro-Borges, P. Corrosion-Induced Cracking of Concrete Elements Exposed to a Natural Marine Environment for Five Years. *Corrosion.* **69** (11), 1122-1131 (2013).
16. Li, D., Wei, R., Du, Y., Guan, X., & Zhou, M. Measurement methods of geometrical parameters and amount of corrosion of steel bar. *Construction & Building Materials.* **154**, 921-927 (2017).
17. Kashani, M. M., Crewe, A. J., & Alexander, N. A. Use of a 3D optical measurement technique for stochastic corrosion pattern analysis of reinforcing bars subjected to accelerated corrosion. *Corrosion Science.* **73** (13), 208-221 (2013).
18. Tang, F., Lin, Z., Chen, G., & Yi, W. Three-dimensional corrosion pit measurement and statistical mechanical degradation analysis of deformed steel bars subjected to accelerated corrosion. *Construction & Building Materials.* **70** (2), 104-117 (2014).
19. Zhang, W., Zhou, B., Gu, X., & Dai, H. Probability Distribution Model for Cross-Sectional Area of Corroded Reinforcing Steel Bars. *Journal of Materials in Civil Engineering.* **26** (5), 822-832 (2013).
20. Wang, X. G., Zhang, W. P., Gu, X. L., & Dai, H. C. Determination of residual cross-sectional areas of corroded bars in reinforced concrete structures using easy-to-measure variables. *Construction & Building Materials.* **38**, 846-853 (2013).
21. Stewart, M. G., & Al-Harthy, A. Pitting corrosion and structural reliability of corroding RC structures: Experimental data and probabilistic analysis. *Reliability Engineering & System Safety.* **93** (3), 373-382 (2008).
22. Darmawan, M. S., & Stewart, M. G. Effect of Spatially Variable Pitting Corrosion on Structural Reliability of Prestressed Concrete Bridge Girders. *Australian Journal of Structural Engineering.* **6** (2), 147-158 (2015).
23. Stewart, M. G., & Mullard, J. A. Spatial time-dependent reliability analysis of corrosion damage and the timing of first repair for RC structures. *Engineering Structures.* **29** (7), 1457-1464 (2007).
24. Kashani, M. M., Lowes, L. N., Crewe, A. J., & Alexander, N. A. Finite element investigation of the influence of corrosion pattern on inelastic buckling and cyclic response of corroded reinforcing bars. *Engineering Structures.* **75**, 113-125 (2014).
25. Apostolopoulos, C. A., Demis, S., & Papadakis, V. G. Chloride-induced corrosion of steel reinforcement - Mechanical performance and pit depth analysis. *Construction and Building Materials.* **38**, 139-146 (2013).
26. Imperatore, S., Rinaldi, Z., & Drago, C. Degradation relationships for the mechanical properties of corroded steel rebars. *Construction and Building Materials.* **148**, 219-230 (2017).
27. Kashani, M. M. Size effect on inelastic buckling behaviour of accelerated pitted 1 corroded bars in porous media. *Journal of Materials in Civil Engineering.* **29** (7) (2017).
28. Meda, A., Mostosi, S., Rinaldi, Z., & Riva, P. Experimental evaluation of the corrosion influence on the cyclic behaviour of RC columns. *Engineering Structures.* **76**, 112-123 (2014).
29. Kashani, M. M., Crewe, A. J., & Alexander, N. A. Structural capacity assessment of corroded RC bridge piers. *Proceedings of the Institution of Civil Engineers - Bridge Engineering.* **170** (1), 28-41 (2017).

30. National Standard of the People's Republic of China. *Standard for test methods of long-term performance and durability of ordinary concrete, Ministry of Housing and Urban-Rural Development of the People's Republic of China, GB/T 50082-2009.* China Construction Industry Press, Beijing 100013, China (2009).

